Comparative Structural Study of the N-Linked Oligosaccharides of Human Normal and Pathological Immunoglobulin G†

Noriko Takahashi* and Ikuko Ishii

Department of Biochemistry, Nagoya City University Medical School, Mizuho-ku Nagoya 467, Japan

Hideko Ishihara, Masami Mori, and Setsuzo Tejima

Department of Hygienic Chemistry, Faculty of Pharmaceutical Sciences, Nagoya City University, Mizuho-ku Nagoya 467, Japan

Royston Jefferis

Department of Immunology, University of Birmingham Medical School, Edgbaston, Birmingham B15 2TJ, U.K.

Satoshi Endo‡ and Yoji Arata‡

Department of Biophysics and Biochemistry, Faculty of Science, University of Tokyo, Hongo, Tokyo 113, Japan

Received July 28, 1986; Revised Manuscript Received October 14, 1986

ABSTRACT: The structures of oligosaccharides of normal and pathological immunoglobulin G (IgG) are reported. Asparagine-linked neutral oligosaccharides were released by *N*-oligosaccharide glycopeptidase (almond) digestion. The reducing ends of the oligosaccharide chains thus obtained were aminated with a fluorescent reagent, 2-aminopyridine, and the mixture of pyridylamino derivatives of the oligosaccharides was separated by reverse-phase high-performance liquid chromatography. It was possible to separate 15 out of the 16 kinds of oligosaccharides that have been suggested to exist in normal human IgG. High-resolution proton nuclear magnetic resonance spectroscopy was used along with chemical methods to determine the structures of the separated oligosaccharides. It has been shown that (1) in normal IgG a biantennary complex-type oligosaccharide with a fucose residue

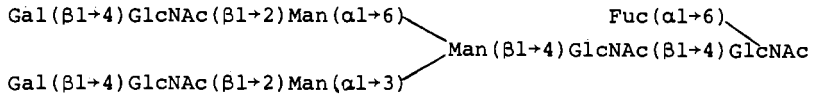

is predominant and (2) four kinds of oligosaccharides, which are biantennary with bisecting *N*-acetylglucosamine and without fucose residues, exist only in a very small quantity. The results obtained for normal IgG were compared with those obtained for three myeloma IgG proteins. It has been found that the most abundant species that exist in the pathological proteins analyzed in the present work lack one or two galactose residues at the nonreducing terminal. We show that the fractions of fucose-containing oligosaccharides are markedly decreased in the heavy-chain disease protein Per. It is of particular interest that in this paraprotein (1) the major component is a biantennary complex-type oligosaccharide that lacks a fucose residue and (2) an oligosaccharide with the structure

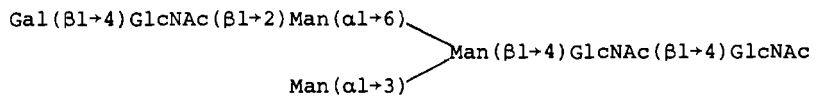

exists as one of the most abundant components.

It is known that human immunoglobulin G (IgG)[1] contains one asparagine-linked oligosaccharide in each of the heavy chains of the F_c portion (Clamp et al., 1964). Mizuochi et al. (1982) have concluded that neutral sugar chains with the structures

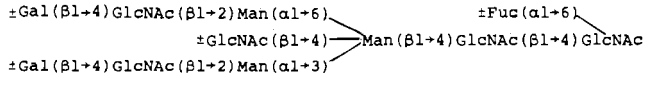

exist in normal human IgG. However, the oligosaccharides reported were separated as three or four peaks by Bio-Gel P-4 column chromatography. Complete isolation of all of the individual oligosaccharides has not yet been accomplished.

In this paper, we report a high-performance liquid chromatography (HPLC)[1] method that gives a *sugar map* representing the distribution of oligosaccharide chains in each sample of IgG. The pattern obtained by HPLC is effective in evaluating the proportion of the amount of each oligosaccharide that is contained in normal and pathological IgG. We will show how differences in the structure of each of the oligosaccharides are clearly reflected on the sugar map. This

† This work was supported in part by the Ministry of Education, Science and Culture of Japan.

‡ Present address: Faculty of Pharmaceutical Sciences, University of Tokyo, Hongo, Tokyo 113, Japan.

[1] Abbreviations: Fuc, L-fucose; Gal, D-galactose; GlcNAc, *N*-acetyl-D-glucosamine; Man, D-mannose; IgG, immunoglobulin G; endo-D, endo-β-*N*-acetylglucosaminidase D; HCD, heavy-chain disease; HPLC, high-performance liquid chromatography; NMR, nuclear magnetic resonance; DSS, sodium 4,4-dimethyl-4-silapentane-1-sulfonate; ppm, parts per million.

0006-2960/87/0426-1137$01.50/0

technique is especially useful in analyzing the presence or absence of an α-L-fucosyl residue and/or the bisecting *N*-acetylglucosamine residue in the oligosaccharide molecules.

High-resolution ^{1}H NMR has been employed for the structural analyses of the oligosaccharide molecules. We will show on the basis of ^{1}H NMR measurements and endo-D digestion experiments that an unsubstituted Man(α1→3)Manβ sequence, which has not yet been reported for human IgG proteins, exists at the nonreducing terminal of one of the oligosaccharide chains that exist in a heavy-chain disease (HCD) protein.

Materials and Methods

Enzymes and Standard Oligosaccharides. *N*-Oligosaccharide glycopeptidase from almond (obtainable as glycopeptidase A), endo-β-*N*-acetylglucosaminidase D from *Diplococcus pneumoniae*, and β-*N*-acetylhexosaminidase were purchased from Seikagaku Kogyo. α-L-Fucosidase from bovine kidney was purchased from Boehringer Mannheim Biochemicals. Neuraminidase from *Arthrobacter ureafaciens* was purchased from Nakarai Chemicals. Pepsin was purchased from Sigma. Standard oligosaccharides described below were prepared by the method of Hotta et al. (1985); biantennary oligosaccharide with fucose was prepared from porcine thyroglobulin (the generous gift of Dr. O. Tarutani, Gunma University); biantennary oligosaccharide without fucose was from fibrinogen. The oligosaccharides obtained were reductively aminated with a fluorescent reagent, 2-aminopyridine, by use of sodium cyanoborohydride. The pyridylamino derivatives of oligosaccharides thus prepared were purified by gel filtration on a Sephadex G-15 column by the method of Hase et al. (1984).

Other Chemicals. The following materials were purchased from the sources indicated: Sephadex G-15 was from Pharmacia; Bio-Gel P-4 (200–400 mesh) was from Bio-Rad; sodium cyanoborohydride was from Aldrich; 2-aminopyridine was from Wako Pure Chemical Industries.

Preparation of Human Normal and Pathological IgG. Human polyclonal IgG proteins were obtained from United States Biochemical Corp. IgG1 proteins Yot, Ogo, and Ike-N were isolated from the sera of patients with multiple myeloma as described previously (Endo & Arata, 1985; Arata et al., 1980). HCD Per was isolated from the urine of a patient with heavy-chain disease and characterized as an IgG1 HCD protein [Jaafar et al. (1983) and references cited therein].

Preparation of Oligosaccharides from IgG. IgG samples of 50–100 mg each were used for the isolation of oligosaccharides. IgG was desialylated by mild acid hydrolysis at pH 2, 90 °C for 1 h. In the case of HCD Per, the intact protein (50 mg) was desialylated with 50 μL of neuraminidase (100 milliunits) in 450 μL of 10 mM citrate–phosphate buffer (pH 5.0) at 37 °C for 16 h. Sialic acid thus released was quantitated by the thiobarbituric acid method (Warren, 1959). Desialylated and pepsin-digested IgG glycopeptides were treated with *N*-oligosaccharide glycopeptidase as described previously (Hotta et al., 1985). The oligosaccharide fraction was collected by gel filtration on a Bio-Gel P-4 column and further purified by passing it through columns of ion-exchange resins Dowex 50WX8 (H^+) and Amberlite IRA-400 (CO_3^{2-}) (Nishibe & Takahashi, 1981).

Isolation of Pyridylamino Oligosaccharides by HPLC. Oligosaccharide fractions obtained as above were reductively aminated with 2-aminopyridine by the use of sodium cyanoborohydride (Hase et al., 1984). The pyridylamino derivatives of oligosaccharides thus prepared were purified by gel filtration on a Sephadex G-15 column and were fractionated and identified by HPLC on a Shim-Pack CLC-ODS column (6 × 150 mm; Shimadzu) according to the method of Hotta et al. (1985).

Other Analytical Procedures. The total amount of neutral sugars was determined by the orcinol–H_2SO_4 reaction (Francois et al., 1962). The IgG preparations were hydrolyzed by 2.5 M trifluoroacetic acid at 100 °C for 6 h in an evacuated sealed tube (Arakawa et al., 1976). The monosaccharides obtained were analyzed by HPLC on a ISA-07/S2504 column (4 × 250 mm) as described by Mikami and Ishida (1983).

^{1}H NMR Measurements. Prior to NMR measurements pyridylamino derivatives of each oligosaccharide (about 10–200 μg each as neutral sugar) isolated by HPLC were desalted by gel filtration on a Sephadex G-15 column. Samples were dissolved in 99.8% D_2O, lyophilized, and dissolved again in 99.8% D_2O at concentrations of 150–700 μM. NMR measurements were made on a Bruker WM-400 spectrometer operating at 400 MHz in the Fourier transform mode. Measurements were made at 23, 30, and 60 °C. Typically, 2000 transients were accumulated for each measurement. Chemical shifts are expressed in parts per million (ppm) from internal DSS but were actually measured by use of internal acetone. The chemical shift of acetone in reference to internal DSS was determined to be 2.216, 2.216, and 2.213 ppm in D_2O at 23, 30, and 60 °C, respectively. Chemical shift values reported are accurate to 0.002 ppm. For the present NMR study, the pyridylamino derivatives of oligosaccharides were used. We have previously shown that residues other than GlcNAc-2 and Man-3 do not show any significant shift upon modification GlcNAc-1 (Takahashi et al., 1986).

Results and Discussion

Preparation of the Sugar Map of IgG. The glycopeptidase cleaves quantitatively β-aspartyl-*N*-acetylglucosamine linkages in glycopeptides, releasing a carbohydrate chain with chitobiose at the reducing end and leaving behind a carbohydrate-free peptide (Takahashi, 1977; Takahashi & Nishibe, 1981). The enzyme has a broad specificity with respect to the carbohydrate moiety. Nonsialylated complex-type oligosaccharides, as well as high-mannose-type and hybrid-type oligosaccharides, have been shown to be released from a variety of glycopeptides (Tarentino & Plummer, 1982; Ishihara et al., 1983; Hotta et al., 1985; Takahashi et al., 1986). By *N*-oligosaccharide glycopeptidase digestion, more than 90% of the total carbohydrates that are contained in the IgG were actually recovered. Typically about 20% are lost during the coupling reaction with 2-aminopyridine and sodium cyanoborohydride (Hase et al., 1984). The mixture of pyridylamino derivatives of the oligosaccharides thus obtained was analyzed by HPLC. The chromatographic recovery of the oligosaccharides in each case was 90–100% of those applied to the column. The area of each peak reflects the mole number of the oligosaccharide.

Oligosaccharides from Normal Human IgG. Figure 1 shows the sugar map of IgG obtained from the pooled sera of normal individuals. Under the optimum chromatographic condition for gradient elution, 15 oligosaccharides can be separated. Oligosaccharides on the map that is given in Figure 1 are divided into the four groups I, II, III, and IV.

The neutral sugar composition of each of pyridylamino derivatives A–H and M–P was determined after hydrolysis with 4 M trifluoroacetic acid at 100 °C for 3 h in an evacuated sealed tube, and the resultant monosaccharides were analyzed by HPLC. The results are summarized in Table I. It was confirmed that each of the fractions contains a sufficiently homogeneous oligosaccharide. The structure of each of the oligosaccharide derivatives separated by the HPLC procedure

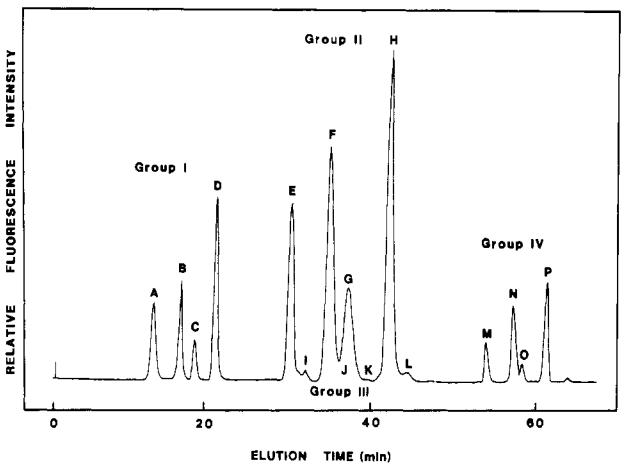

FIGURE 1: HPLC profile of pyridylamino derivatives of oligosaccharides of IgG from normal individuals. Oligosaccharide fractions obtained by glycopeptidase digestion of the peptic peptides of IgG were aminated and subjected to HPLC analyses as described in the text. Symbols: G, galactose; M, mannose; F, fucose; GN, *N*-acetylglucosamine. Peak P, for example, represents

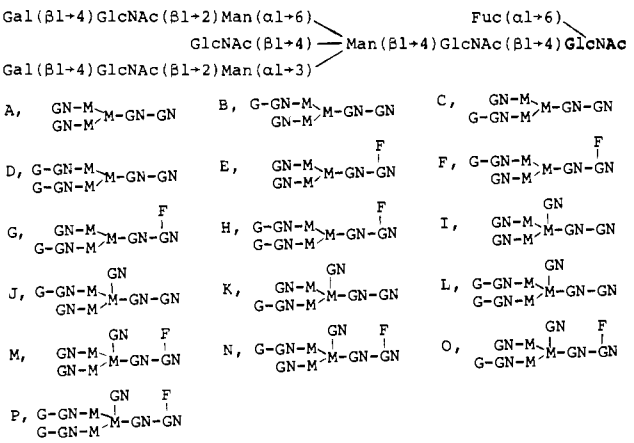

Table I: Neutral Sugar Composition of Each of the Oligosaccharide Derivatives Separated by HPLC

group	compd	molar ratio		
		Man[a]	Fuc	Gal
I	A	3.0	0	0.10
	B	3.0	0	1.16
	C	3.0	0	1.02
	D	3.0	0	2.09
II	E	3.0	1.12	0.21
	F	3.0	1.09	0.97
	G	3.0	1.05	0.92
	H	3.0	0.88	1.89
IV	M	3.0	1.15	0.15
	N	3.0	0.98	1.06
	O	3.0	0.87	1.11
	P	3.0	1.23	2.01

[a] Molar ratios were calculated by taking the value of mannose as 3.0.

was elucidated on the basis of the results obtained by chemical analyses and ^{1}H NMR measurements. It was concluded that group I (A–D), group II (E–H), group III (I–L), and group IV (M–P) correspond to oligosaccharides that are biantennary without fucose, biantennary with fucose, biantennary with bisecting *N*-acetylglucosamine and without fucose, and biantennary with bisecting *N*-acetylglucosamine and with fucose, respectively. Assignments of structures to each of these oligosaccharides are summarized in the caption of Figure 1. The combined fractions for each of the oligosaccharides of the four groups I, II, III, and IV were estimated at 21%, 67%, ≲1%, and 11%, respectively.

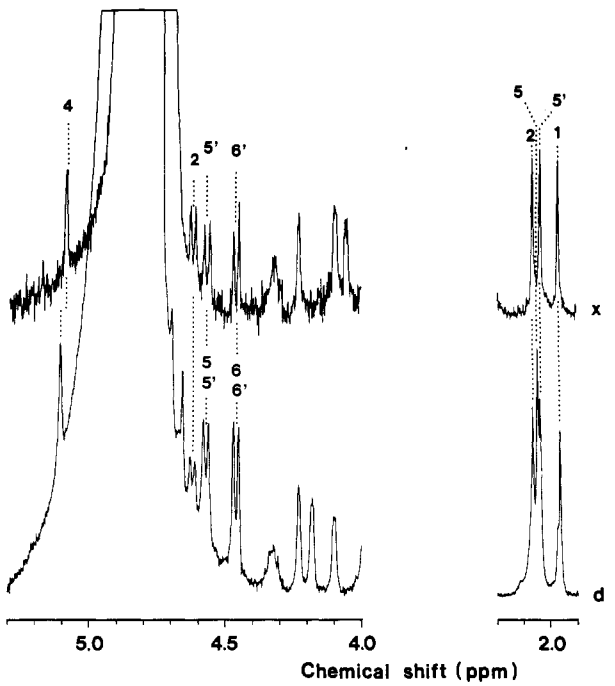

FIGURE 2: 400-MHz ^{1}H NMR spectra of anomeric (left) and methyl (right) protons of oligosaccharide D from normal human IgG (d) and oligosaccharide X from HCD Per (x). Assignments: 4, Man-4; 2, GlcNAc-2; 5, GlcNAc-5; 5′, GlcNAc-5′; 6, Gal-6; 6′, Gal-6′. The free-induction decay was recorded with 16K data points and a spectral width of ±2500 Hz. Typically, 1000 transients were acquired, and a line broadening of 0.3 Hz was applied prior to Fourier transformation. The probe temperatures were 23 (d) and 30 °C (x).

In the following we summarized how the structure of each oligosaccharide was determined on the basis of chemical analyses and ^{1}H NMR data.

Group I (Peaks A–D). A ^{1}H NMR spectrum of peak D is reproduced in Figure 2. The ^{1}H NMR spectral data for the H-1 and acetyl group clearly indicate that oligosaccharides A–D do not possess Fuc and bisecting GlcNAc (GlcNAc-9). (See Table II.) Oligosaccharides B and C possess one Gal at a nonreducing end. The H-1 chemical shifts for GlcNAc-5 and GlcNAc-5′ become 4.572 and 4.570 ppm, respectively, when Gal is bonded to these GlcNAc residues. However, the H-1 proton gives identical chemical shifts for the two GlcNAc residues. Therefore, the H-1 chemical shift data do not give any information concerning the structure of oligosaccharides B and C. It should, however, be noted that the chemical shifts for the acetyl group of oligosaccharides A–D are different for GlcNAc-5 and GlcNAc-5′. The chemical shift for GlcNAc-5 does not change at all even when Gal is bonded to it. By contrast, linkage of Gal to GlcNAc-5′ gives rise to a small but significant shift; i.e., the chemical shift for GlcNAc-5′ is shifted from 2.041 (A) to 2.038 (B) ppm and from 2.040 (C) to 2.037 (D) ppm. This means that oligosaccharides B and D possess Gal bonded to GlcNAc-5′. We therefore conclude that oligosaccharide C has Gal linked to GlcNAc-5. The H-1 chemical shift for Man-4′ is shifted significantly to low field upon addition of Gal-6′. (See Table II.) These data are also consistent with the above conclusion about the assignment of the structures of oligosaccharides B and C. The linkage position for B and C was further confirmed by a chemical procedure as described below for oligosaccharides F and G.

Group II (Peaks E–H). Oligosaccharides E–H (group II) and I–L (group III) were collected as a mixture (Figure 3, profile 1) and digested with α-L-fucosidase. About 100 milliunits of the enzyme was used for 1 nmol of the substrate. The reaction mixture was again subjected to the HPLC pro-

Table II: Chemical Shifts of Anomeric Protons and Methyl Protons for the Pyridylamino Derivatives of Oligosaccharides of Human Normal IgG and Myeloma IgG

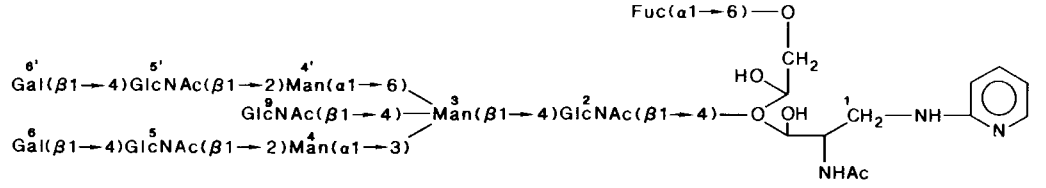

compd	chemical shifts[a] of anomeric protons: Glc-NAc-2	Man-3	Man-4	Man-4′	Glc-NAc-5	Glc-NAc-5′	Gal-6	Gal-6′	Glc-NAc-9	Fuc	chemical shifts[a] of methyl protons: Glc-NAc-2	Glc-NAc-5	Glc-NAc-5′	Glc-NAc-9	Fuc
normal IgG															
A	4.620	(4.747)[b]	5.107	(4.903)	4.545	4.545					2.061	2.048	2.041		
B	4.620	(4.745)	5.108	(4.911)	4.547	4.570		4.462			2.065	2.049	2.038		
C	4.624	(4.745)	5.107	(4.907)	4.572	4.548	4.462				2.063	2.047	2.040		
D	4.621	(4.746)	5.110	(4.912)	4.572	4.572	4.461	4.461			2.065	2.047	2.037		
E	4.710	(4.749)	5.106	4.909 (4.899)	4.545	4.545				(4.839)	2.073	2.048	2.042		1.171
F	4.680	(4.747)	5.107	4.915 (4.907)	4.547	4.570		4.462		(4.846)	2.074	2.048	2.038		1.175
G	4.687	(4.749)	5.108	4.909 (4.900)	4.567	4.547	4.460			(4.843)	2.073	2.046	2.042		1.172
H	4.675	(4.749)	5.110	4.916 (4.909)	4.573	4.573	4.461	4.461		(4.848)	2.075	2.047	2.037		1.178
M	c	(4.695)	5.052	4.983 (4.977)	4.547	4.536			4.454	(4.850)	2.073	2.054	2.040	2.064	1.175
N	4.673	(4.690)	5.054	4.996 (4.985)	4.550	4.570		4.467	4.456	(4.850)	2.078	2.052	2.032	2.064	1.172
O	c	(4.691)	(5.048)	(4.977)	c	c	c	c	c	(4.848)	2.072	2.050	2.039	2.060	1.173
P	4.670	(4.686)	5.049	4.992 (4.982)	4.570	4.570	4.462	4.462	4.462	(4.852)	2.078	2.048	2.032	2.060	1.176
Yot															
E	c	c	5.108	c	c	c	c	c	c	c	2.072	2.046	2.042		c
F + G	c	c	5.108	c	[4.571,	4.547][d]		[4.464]	c	c	2.073	2.047	2.038		1.171
H	c	c	5.111	4.913	4.573	4.573	4.461	4.461	c	c	2.075	2.046	2.038		1.173
M–P	c	c	5.051	4.991	c	c	c	c	c	c	2.076	2.052	2.040	2.062	c
Ogo															
E	c	c	5.107	4.905	4.545	4.545			c	c	2.072	2.048	2.042		1.171
M–P	c	c	5.050	4.983	c	c	c	c	c	c	2.072	2.054	2.040	2.063	1.169
Ike-N															
E	c	c	5.108	4.905	4.546	4.546	c	c	c	c	2.072	2.048	2.042		1.171
F + G	c	c	5.107	4.905	c	c		[4.462]	c	c	2.073	2.047	2.040		1.171
M–P	c	c	5.052	4.979	c	c	c	c	c	c	2.071	2.053	2.040	2.062	c
HCD Per															
B	4.625	(4.745)	5.109	(4.909)	4.548	4.571		4.462			2.064	2.047	2.036		
X	4.620	(4.743)	5.089	(4.907)		4.570		4.462			2.064		2.035		
D	4.624	(4.744)	5.113	(4.909)	4.573	4.573	4.462	4.462			2.064	2.046	2.037		

[a] Chemical shifts are expressed in ppm from internal DSS but were actually measured with internal acetone (δ = 2.216 ppm in D_2O at 23 °C) for normal IgG and with internal acetone (δ = 2.216 ppm in D_2O at 30 °C) for myeloma IgG and HCD Per. [b] Values in parentheses were measured at 60 °C by using internal acetone (δ = 2.213 ppm in D_2O). [c] The signal was not detectable due to the limited amount of sample. [d] Use of the mixture of F + G made it impossible to differentiate 5 and 5′ and 6 and 6′.

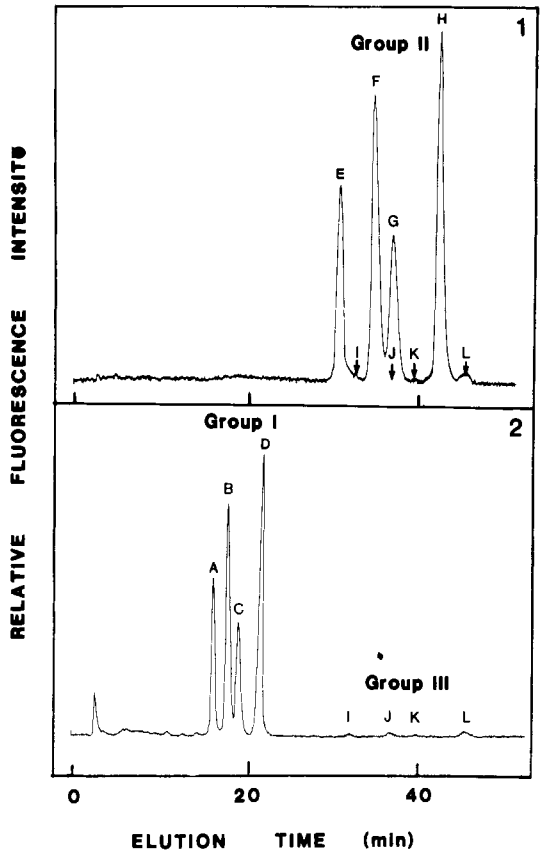

FIGURE 3: Separation by HPLC procedure of oligosaccharides of group III from those of group II: (1) oligosaccharide derivatives E–L separated by the HPLC procedure; (2) oligosaccharides corresponding to fractions E–L collected and digested with α-L-fucosidase and again subjected to HPLC analysis. Peaks E, F, G, and H are shifted to the positions of A, B, C, and D, respectively, and I–L remain at the original positions.

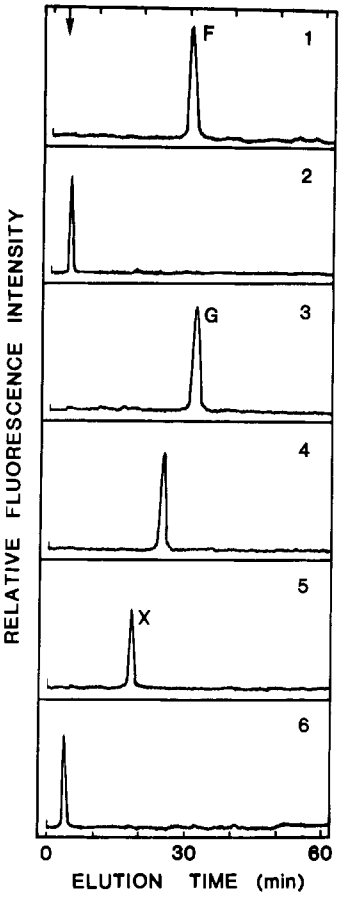

FIGURE 4: HPLC analyses of endo-D digestion of oligosaccharides F and G from normal IgG and of oligosaccharide X from HCD Per: (1) intact oligosaccharide F from normal IgG; (2) oligosaccharide F (1 nmol) sequentially digested with 40 milliunits each of β-*N*-acetylglucosaminidase (*Charonia lampas*) and endo-D; (3) intact oligosaccharide G from normal IgG; (4) oligosaccharide G sequentially digested with two enzymes under the same conditions as in the case of oligosaccharide F; (5) intact oligosaccharide X from HCD Per; (6) oligosaccharide X digested with endo-D directly at the same conditions as above. The arrow indicates the position of the standard pyridylamino derivative of *N*-acetylglucosamine.

cedure. As Figure 3 clearly shows, peaks E, F, G, and H are shifted and superimposed on peaks A, B, C, and D, respectively, whereas peaks I–L remain at their original positions. This result clearly indicates that oligosaccharides of group II have an α-fucosyl residue bonded to each of oligosaccharides of group I. One galactose residue exists in both oligosaccharides F and G. Each 1 nmol of oligosaccharides F and G was sequentially digested with 40 milliunits of β-*N*-acetylglucosaminidase at pH 5.0 and then with 40 milliunits of endo-β-*N*-acetylglucosaminidase D (endo-D) at pH 6.5, and the reaction products were analyzed again by the HPLC procedure. The sugar residue essential for the action of endo-D has been identified as an unsubstituted α-mannosyl residue linked to the innermost β-mannosyl residue by α1→3 linkage (Tai et al., 1975). Since galactosyl-*N*-acetylglucosaminyl chains hinder the action of endo-D, removal of *N*-acetylglucosamine in advance by exoglycosidase is essential for the endo-D digestion. It was observed that on treatment with *N*-acetylglucosaminidase and endo-D the pyridylamino derivative of oligosaccharide F disappears and a new peak appears instead at a position that coincides with that of the pyridylamino derivative of GlcNAc. (See Figure 4, profiles 1 and 2.) By contrast, it was observed that only nonreducing terminal GlcNAc can be deleted from oligosaccharide G (Figure 4, profiles 3 and 4). The results of these experiments indicate that, in oligosaccharides F and G, galactose is bonded to the Man(α1→6)Manβ branch and the Man(α1→3)Manβ branch, respectively.

Figure 5 shows ^{1}H NMR spectra of oligosaccharides E–H. The CH_3 and H-1 proton resonances due to fucose are observed for all the oligosaccharides. The NMR data also indicate that these oligosaccharides do not possess a bisecting GlcNAc. The NMR measurements indicate that oligosaccharide H has two Gal residues at the nonreducing terminal, whereas both Gal residues are missing in oligosaccharide E. The chemical shifts for the acetyl group are separately observed for GlcNAc-5 and GlcNAc-5′. No significant change of the chemical shifts of the acetyl protons of GlcNAc-5 is observed for oligosaccharides E–H. In the case of oligosaccharides F and H, the acetyl protons of GlcNAc-5′ give rise to a significant high-field shift. These NMR data are quite consistent with those obtained by the chemical analyses that have been described above.

As Figure 1 shows, the major component for normal human IgG is Gal(β1→4)GlcNAc(β1→2)Man(α1→6)[Gal(β1→4)GlcNAc(β1→2)Man(α1→3)]Man(β1→4)GlcNAc(β1→4)[Fuc(α1→6)]GlcNAcβ (peak H).

Group III (Peaks I–L). Although oligosaccharides of this group are quite small in quantity, peaks I, K, and L were detectable on the sugar map (Figure 1) under chromatographic conditions routinely used. The result shown in Figure 3 clearly shows that oligosaccharides of group III can be separated from those of group II. It was therefore possible to observe and quantitate the oligosaccharides of group III. It was observed that the signal with a chemical shift of 1.18 ppm corresponding

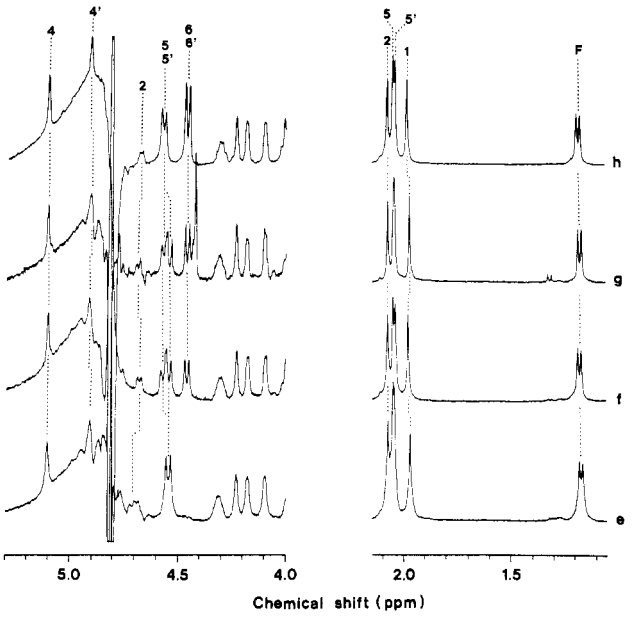

FIGURE 5: 400-MHz ^{1}H NMR spectra of anomeric (left) and methyl (right) protons of oligosaccharides E (e), F (f), G (g), and H (h) from normal human IgG. Assignments: 4, Man-4; 4′, Man-4′; 2, GlcNAc-2; 5, GlcNAc-5; 5′, GlcNAc-5′; 6, Gal-6; 6′, Gal-6′; F, Fuc. Spectral conditions are as described in Figure 2. The probe temperature was 30 °C.

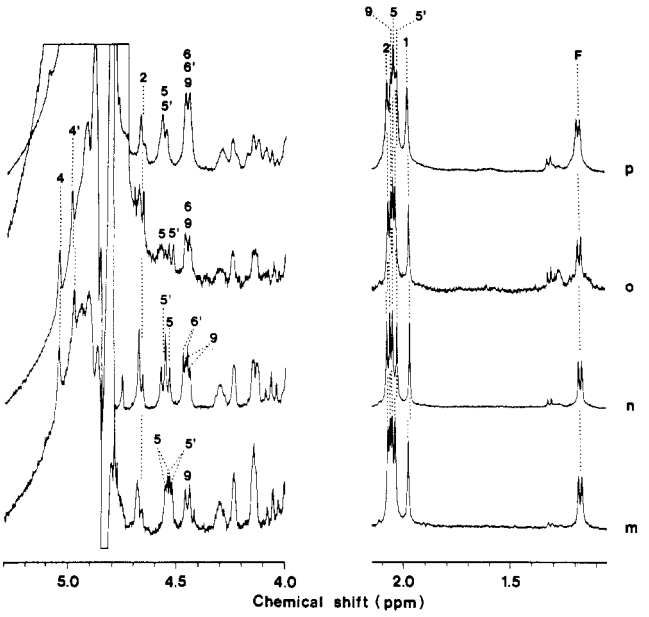

FIGURE 6: 400-MHz ^{1}H NMR spectra of anomeric (left) and methyl (right) protons of oligosaccharides M (m), N (n), O (o), and P (p) from normal human IgG. Assignments: 4, Man-4; 4′, Man-4′; 2, GlcNAc-2; 5, GlcNAc-5; 5′, GlcNAC-5′; 6, Gal-6; 6′, Gal-6′; 9, GlcNAc-9; F, Fuc. Spectral conditions are as described in Figure 2. The probe temperature was 30 °C.

to the CH_3 of α-fucosyl residue is missing in oligosaccharides of group III. As we describe below, oligosaccharides M–P can be converted to oligosaccharides I–L on treatment with α-L-fucosidase. On the basis of these results, we propose the structures of oligosaccharides I–L as shown in the caption of Figure 1.

Group IV (Peaks M–P). In the methylation analysis of oligosaccharides M–P, 2-*O*-methylmannose was obtained from each of these oligosaccharides instead of 2,4-di-*O*-methylmannose. Furthermore, it was observed that, on incubation for 3 h with 100 milliunits of α-L-fucosidase, each 1 nmol of oligosaccharides M, N, O, and P was converted to smaller

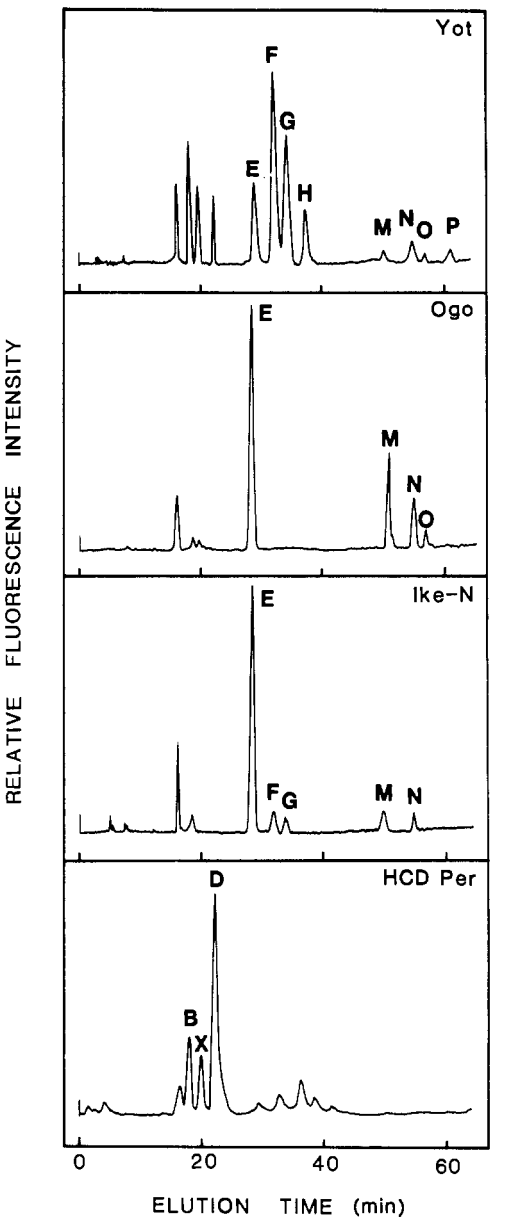

FIGURE 7: Comparison of oligosaccharide profiles from human IgG by HPLC: Yot, Ogo, and Ike-N, from the sera of patients with multiple myeloma; HCD Per, from the urine of a patient with heavy-chain disease.

oligosaccharides, which gave the same eluting positions as oligosaccharides I, J, K, and L, respectively. This indicates that bisecting GlcNAc is bonded to β-mannose in oligosaccharides M–P. This result was confirmed by NMR measurements. Figure 6 gives ^{1}H NMR spectra of oligosaccharides M–P. Oligosaccharides M–P all give a peak at 2.06 ppm, which is due to an acetyl group of bisecting GlcNAc. Oligosaccharides M–P give a CH_3 peak for Fuc at 1.172–1.176 ppm. Signals for the acetyl groups of GlcNAc-5, GlcNAc-5′, and GlcNAc-9 are separately observed in these oligosaccharides. As in the cases of oligosaccharides A–D and E–H, the GlcNAc-5′ signals are significantly shifted by the introduction of Gal to the nonreducing end. This indicates that oligosaccharides N and O possess Gal linked to GlcNAc-5′ and GlcNAc-5, respectively.

Sugar Map of Myeloma IgG. Figure 7 shows the oligosaccharide profiles of paraproteins isolated from patients with multiple myeloma (Yot, Ogo, and Ike-N) and with heavy-chain disease (HCD Per). The main characteristic of the profiles for proteins Yot and Ike-N is a dramatic decrease in

quantity of oligosaccharide H, which is the major component in the case of normal IgG. It was also observed that the fraction of oligosaccharide E, which lacks two galactose residues, is markedly increased. Furthermore, the amount of oligosaccharides with bisecting GlcNAc is larger in protein Ogo than that observed for other IgG proteins examined. In proteins Yot and Ogo, fractions of the oligosaccharides with bisecting GlcNAc were 7.4 and 33.1, respectively. Fractions of the oligosaccharides with fucose were 71.4 and 84.9 for proteins Yot and Ogo, respectively. These results are in good agreement with those obtained by Mizuochi et al. (1982) with hydrazinolysis, using the same samples (proteins Yot and Ogo), where fractions of molecules with bisecting GlcNAc were 7.8% and 28.8%, respectively, and those of molecules with fucose 75.2% and 85.8%, respectively. Oligosaccharides E, F + G, H, and M–P in protein Yot and oligosaccharides E and M–P in proteins Ogo and Ike-N give chemical shifts that are consistent with the proposed structures (Table II).

Oligosaccharide Profile of HCD Per. About 300 μg of HCD Per was hydrolyzed in 0.5 mL of 2.5 M trifluoroacetic acid at 100 °C for 6 h. The composition of neutral sugars thus obtained was determined by HPLC. The molar ratio Man:Gal:Fuc = 3.0:2.4:0.3 was obtained. This ratio is quite different from 3.0:1.3:0.98 obtained for normal IgG. The oligosaccharide fraction obtained by glycopeptidase digestion of HCD Per was separated by Bio-Gel P-4 column chromatography and was desalted by passage through ion-exchange resins. The pyridylamino derivative of the oligosaccharide fraction was subjected to HPLC (Figure 7).

The result of ^{1}H NMR analyses clearly indicates that the major component of HCD Per, fraction D in Figure 7, is a biantennary complex-type oligosaccharide without a fucose residue. The structure of this oligosaccharide is the same as that of oligosaccharide D on the sugar map of normal IgG (Table II). On the basis of comparison of the chemical shift data listed for HCD Per with those for normal IgG, we conclude that fraction B of HCD Per (Figure 7) corresponds to oligosaccharide B on the sugar map of normal IgG. Oligosaccharide X was fractionated by HPLC as shown in Figure 7. In Figure 2 a ^{1}H NMR spectrum of oligosaccharide X is compared with that of oligosaccharide D. The NMR data clearly indicate that oligosaccharide X does not possess GlcNAc-5 and therefore Gal-6. Correspondingly, the Man-4 exhibits a chemical shift that is higher than in the case of oligosaccharide D. This result also confirms that there is no substitution at Man-4. The chemical shift data (Table II) indicate that fraction X has the structure Gal(β1→4)-GlcNAc(β1→2)Man(α1→6)[Man(α1→3)]Man(β1→4)-GlcNAc(β1→4)GlcNAc. In order to confirm the structure of this oligosaccharide, 1 nmol of the pyridylamino derivative of oligosaccharide X was digested directly with 40 milliunits of endo-D at pH 6.5. It was observed by an HPLC procedure that oligosaccharide X disappeared and the pyridylamino derivative of GlcNAc appeared instead after the incubation with endo-D (Figure 4, profiles 5 and 6). This result clearly indicates that the Man(α1→3) residue is unsubstituted in oligosaccharide X.

The present results indicate that HCD protein Per possesses an oligosaccharide that has not been shown to exist in normal IgG in any detectable amount. The structure of oligosaccharide X is identical with that obtained from newborn meconium (Herlant-Peers et al., 1981) and from urine from patients with Morquio syndrome type B (Michalski et al., 1982). In the latter two cases, however, the oligosaccharide preparation is a mixture of two isomeric structures, one having the NeuAc(α2→6)Gal(β1→4)GlcNAc(β1→2) unit linked to Man-4 and the other linked to Man-4′, which is the same as in oligosaccharide X. There is a possibility that the oligosaccharides found in human meconium are products of the catabolism of glycoproteins. In recent publications, Yamashita et al. (1983) and Hase et al. (1986) demonstrated that the two kinds of oligosaccharides also exist in hen ovomucoid and in Japanese quail ovomucoid, respectively. It should be noted that, in the case of HCD Per examined in this work, only oligosaccharide X exists and the isomeric oligosaccharide with Gal(β1→4)GlcNAc linked to the Man(α1→3) branch cannot be detected. Physiological significance of the results obtained will be the subject of a future study.

ACKNOWLEDGMENTS

N.T. is greatly indebted to Dr. Ryo Tanaka of Nagoya City University for his helpful discussion. We thank C. Iwata for her excellent technical assistance. We gratefully acknowledge generous considerations by Dr. H. Hanssum and S. Ueki of Bruker Japan for the use of their WM-400 spectrometer.

Registry No. A, 106212-99-1; B, 106230-72-2; C, 106213-00-7; D, 89243-14-1; E, 106213-01-8; F, 106230-73-3; G, 106213-02-9; H, 106230-74-4; I, 106213-05-2; J, 106249-98-3; K, 106213-03-0; L, 106230-75-5; M, 106213-04-1; N, 106230-76-6; O, 106213-06-3; P, 106230-77-7; G-GN-M-M(M)-GN-GN, 106212-98-0.

REFERENCES

Arakawa, Y., Imanari, T., & Tamura, Z. (1976) *Chem. Pharm. Bull. 24*, 2032–2037.

Arata, Y., Honzawa, M., & Shimizu, A. (1980) *Biochemistry 19*, 5130–5135.

Clamp, J. R., Bernier, G. M., & Putnam, F. W. (1964) *Biochim. Biophys. Acta 86*, 149–155.

Endo, S., & Arata, Y. (1985) *Biochemistry 24*, 1561–1568.

Francois, C., Marshall, R. D., & Neuberger, A. (1962) *Biochem. J. 83*, 335–341.

Hase, S., Ibuki, T., & Ikenaka, T. (1984) *J. Biochem. (Tokyo) 95*, 197–203.

Hase, S., Sugimoto, T., Takemoto, H., Ikenaka, T., & Schmid, K. (1986) *J. Biochem. (Tokyo) 99*, 1725–1733.

Herlant-Peers, M.-C., Montreuil, J., Strecker, G., Dorland, L., van Halbeek, H., Veldink, G. A., & Vliegenthart, J. F. G. (1981) *Eur. J. Biochem. 117*, 291–300.

Hotta, T., Ishii, I., Ishihara, H., Tejima, S., Tarutani, O., & Takahashi, N. (1985) *J. Appl. Biochem. 7*, 98–103.

Ishihara, H., Tejima, S., Takahashi, N., Takayasu, T., & Shinoda, T. (1983) *Biochem. Biophys. Res. Commun. 110*, 181–186.

Jaafar, M. I. N., Lowe, J. A., Ling, N. R., & Jefferis, R. (1983) *Mol. Immunol. 20*, 679–686.

Michalksi, J.-C., Strecker, G., van Halbeek, H., Dorland, L., & Vliegenthart, J. F. G. (1982) *Carbohydr. Res. 100*, 351–363.

Mikami, H., & Ishida, Y. (1983) *Bunseki Kagaku 32*, E207–E210.

Mizuochi, T., Taniguchi, T., Shimizu, A., & Kobata, A. (1982) *J. Immunol. 129*, 2016–2020.

Nishibe, H., & Takahashi, N. (1981) *Biochim. Biophys. Acta 661*, 274–279.

Tai, T., Yamashita, K., Arakawa, M., Koide, N., Muramatsu, T., Iwashita, S., Inoue, Y., & Kobata, A. (1975) *J. Biol. Chem. 250*, 8569–8575.

Takahashi, N. (1977) *Biochem. Biophys. Res. Commun. 76*, 1194–1201.

Takahashi, N., & Nishibe, H. (1981) *Biochim. Biophys. Acta 657*, 457–467.

Takahashi, N., Hotta, T., Ishihara, H., Mori, M., Tejima, S., Bligny, R., Akazawa, T., Endo, S., & Arata, Y. (1986) *Biochemistry 25*, 388-395.
Tarentino, A. L., & Plummer, T. H., Jr. (1982) *J. Biol. Chem. 257*, 10776-10780.
Vliegenthart, J. F. G., Dorland, L., & van Halbeek, H. (1983) *Adv. Carbohydr. Chem. Biochem. 41*, 209-374.
Warren, L. (1959) *J. Biol. Chem. 234*, 1971-1975.
Yamashita, K., Kammerling, J. P., & Kobata, A. (1983) *J. Biol. Chem. 258*, 3099-3106.

Structural Similarities among Valine-Accepting tRNA-like Structures in Tymoviral RNAs and Elongator tRNAs

Alex van Belkum, Jiang Bingkun, Krijn Rietveld, Cornelis W. A. Pleij,* and Leendert Bosch
Department of Biochemistry, University of Leiden, 2333 AL Leiden, The Netherlands
Received June 2, 1986; Revised Manuscript Received October 6, 1986

ABSTRACT: A spatial model for the tRNA-like structure at the 3′ terminus of TYMV RNA has been proposed previously on the basis of chemical and enzymatic structure mapping studies [Rietveld, K., van Poelgeest, R., Pleij, C. W. A., van Boom, J. H., & Bosch, L. (1982) *Nucleic Acids Res. 10*, 1929-1946]. In this paper we describe the determination of the primary structure at the 3′ end of a number of tymoviral RNAs. Sequence comparison shows that the RNAs from CYVV, EMV, APLV, KYMV, and OYMV can adopt secondary and tertiary structures that fit the model as proposed for TYMV RNA. The pseudoknot formation that is essential for the construction of the aminoacyl acceptor arm of TYMV RNA is conserved in all tymoviral RNAs studied. The length of the individual double-helical segments coaxially stacked in this arm can vary and is well correlated with established tymoviral relationships. When the consensus structure of the valine-accepting tRNA-like structures is compared to that of standard $tRNA^{Val}$s, some striking similarities are observed. Only a limited number of nucleotides, located at defined positions, appear to be conserved. An ACA(C) sequence in the anticodon loop probably is the major structural feature responsible for the specific recognition of the cognate valyl-tRNA synthetase.

Tymoviruses are small icosahedral plant viruses, infecting a large number of dicotyledonous plants in most parts of the world (Guy et al., 1984). Viral preparations characteristically contain two major types of particles, both with a diameter of 25-30 nm. The faster sedimenting particle (115 s) or bottom component contains the genomic RNA (M_r 2.0 × 10^6) while the slower sedimenting particle (55 S) or top component is devoid of RNA and consists of the empty protein shell. Classification of the 16 tymoviruses described to date is based on either serological relationships (Koenig, 1976), amino acid composition of the coat protein (Paul et al., 1980), or host range (Guy et al., 1984). For recent reviews on the biological and structural properties and the classification of tymoviruses, see Matthews (1981) and Koenig and Lesemann (1979, 1981).

The genomic RNA of turnip yellow mosaic virus (TYMV), the type member of the tymovirus group, was the first viral RNA shown to possess a 3′ terminus that can be specifically aminoacylated, pointing to the presence of a tRNA-like structure (Hall, 1979; Haenni et al., 1982). TYMV RNA can be charged, like some other tymoviral RNAs, with valine (Pinck et al., 1970, 1974; Yot et al., 1970).

So far, five different plant virus groups have been reported to accept a specific amino acid at the 3′ end of their genomic RNAs (Joshi et al., 1983; Kozlov et al., 1984). We have proposed spatial models of these tRNA-like structures on the basis of structure mapping studies on 3′-terminal fragments of BMV RNA, TYMV RNA, and TMV RNA [Rietveld et al. (1984) and references cited therein]. The models of the tRNA-like structure of brome mosaic virus RNA and that of tobacco mosaic virus RNA are strongly supported by sequence comparisons with related RNAs from the bromovirus and tobamovirus group, respectively. Apart from a partial sequence of the 3′ terminus of egg plant mosaic virus (EMV) RNA (Briand et al., 1976), such information was not available in the case of the tRNA-like structure of TYMV RNA (Rietveld et al., 1982).

Since a comparative analysis of related RNA sequences can furnish additional evidence for proposed secondary and tertiary structures (Fox & Woese, 1975; Noller, 1984), we have determined the primary structure at the 3′ end of a number of tymoviral RNAs. In this paper we show that the 3′ termini of andean potato latent virus (APLV) RNA, clitoria yellow vein virus (CYVV) RNA, eggplant mosaic virus (EMV) RNA, kennedya yellow mosaic virus (KYMV) RNA, and ononis yellow mosaic virus (OYMV) RNA can be folded in a secondary structure as proposed for TYMV RNA (Rietveld et al., 1982). In addition, it is evident that in the construction of the aminoacyl acceptor arm the principle of pseudoknotting plays an essential role. Interviral comparisons revealed some interesting features of the folding of this domain. Moreover, we have found some common elements in these valine-specific tRNA-like structures on one hand and in the elongator $tRNA^{Val}$s from eukaryotic and prokaryotic organisms on the other. These findings may contribute to our understanding of how tRNAs are specifically recognized by their cognate aminoacyl-tRNA synthetase.

Materials and Methods

Enzymes. An *E. coli* extract containing aminoacyl-tRNA synthetases and CTP,ATP:tRNA nucleotidyltransferase was prepared essentially as described by Joshi et al. (1982a). After the final DEAE-cellulose chromatography step, the preparation was tested for the presence of all aminoacyl-tRNA synthetases, the presence of CTP,ATP:tRNA nucleotidyltransferase, and the absence of endogenous tRNA. CTP,ATP:tRNA nucleotidyltransferase was isolated from bakers' yeast according to

0006-2960/87/0426-1144$01.50/0